J Appl Physiol
90: 1887–1899, 2001.

Oxygen measurements in brain stem slices exposed to normobaric hyperoxia and hyperbaric oxygen

DANIEL K. MULKEY,[1] RICHARD A. HENDERSON III,[2] JAMES E. OLSON,[1,3]
ROBERT W. PUTNAM,[1] AND JAY B. DEAN[1]
[1]*Department of Physiology and Biophysics, Environmental and Hyperbaric Cell Biology Facility,*
[2]*Department of Community Health, and* [3]*Department of Emergency Medicine, College of Science and Mathematics, Wright State University School of Medicine, Dayton, Ohio 45435*

Received 1 November 2000; accepted in final form 29 December 2000

Mulkey, Daniel K., Richard A. Henderson III, James E. Olson, Robert W. Putnam, and Jay B. Dean. Oxygen measurements in brain stem slices exposed to normobaric hyperoxia and hyperbaric oxygen. *J Appl Physiol* 90: 1887–1899, 2001.—We previously reported (*J Appl Physiol* 89: 807–822, 2000) that ≤10 min of hyperbaric oxygen (HBO_2; ≤2,468 Torr) stimulates solitary complex neurons. To better define the hyperoxic stimulus, we measured P_{O_2} in the solitary complex of 300-μm-thick rat medullary slices, using polarographic carbon fiber microelectrodes, during perfusion with media having P_{O_2} values ranging from 156 to 2,468 Torr. Under control conditions, slices equilibrated with 95% O_2 at barometric pressure of 1 atmospheres absolute had minimum P_{O_2} values at their centers (291 ± 20 Torr) that were ~10-fold greater than P_{O_2} values measured in the intact central nervous system (10–34 Torr). During HBO_2, P_{O_2} increased at the center of the slice from 616 ± 16 to 1,517 ± 15 Torr. Tissue oxygen consumption tended to decrease at medium P_{O_2} ≥ 1,675 Torr to levels not different from values measured at P_{O_2} found in all media in metabolically poisoned slices (2-deoxy-D-glucose and antimycin A). We conclude that control medium used in most brain slice studies is hyperoxic at normobaric pressure. During HBO_2, slice P_{O_2} increases to levels that appear to reduce metabolism.

solitary complex; polarographic oxygen measurements; metabolism; reactive oxygen species; central nervous system oxygen toxicity

THE IN VITRO BRAIN SLICE PREPARATION has been used for more then 40 years to study neuronal excitability because it allows considerable control of the neuronal environment while retaining local neuronal circuitry (42). Brain slices are removed from blood supply and receive oxygen solely by diffusion from the nutrient medium that bathes the tissue. To ensure adequate oxygenation of cells lying deep to the slice surface, most brain slice studies use 95% O_2 to set the P_{O_2} in the control medium. At a barometric pressure (P_B) of 1 atmosphere absolute (ATA),[1] this produces a P_{O_2} in the nutrient medium of ~722 Torr. Under this condition, brain slices remain viable for up to 8 h, based on electrophysiological criteria (12). Consequently, it has generally been assumed that P_{O_2} in the core of a submerged slice is adequate (40).

Several studies have reported tissue P_{O_2} values in brain slices measured with polarographic microelectrodes (3–5, 19–21, 28, 50, 56). These experiments were done to determine the slice thickness that optimized slice viability, as measured by extracellularly recorded field potentials, while ensuring that an anoxic tissue core was avoided (19), or, alternatively, to identify the level of oxygenation in the slice so that electrophysiological data could be correlated with tissue P_{O_2} during hypoxia (28, 50, 56) and hyperoxia (3–5, 56). Because P_{O_2} at any depth in a slice is determined by P_{O_2} of the perfusate, oxygen diffusion distance into the slice, and oxygen consumption ($\dot{V}_{O_2}$), tissue P_{O_2} measurements were also used to determine $\dot{V}_{O_2}$ (20, 21). Results from these studies varied, however, because of differences in slice thickness, central nervous system (CNS) regions, animal age, and orientation of slice surfaces relative to the supporting structure (nylon mesh vs. solid Plexiglas support) and the fluid-gas interface (interface slice vs. submerged slice) (4, 19, 28). Nevertheless, under control conditions, 300- to 450-μm-thick brain slices had minimum P_{O_2} values that were consistently higher (19, 20, 28, 50) than those measured in the intact CNS (9, 23, 24, 27, 51, 61).

We studied the effects of hyperoxia, reactive oxygen species (ROS), and antioxidants on the electrophysiology of neurons in the solitary complex (12, 44–46), an important cardiorespiratory control center in the caudodorsal medulla oblongata (14, 18). The challenge of studying hyperoxia in rat brain slices, however, is that the standard control P_{O_2} of the medium used in this preparation is already hyperoxic at normobaric pressure (P_B of ~1 ATA). Increasing tissue P_{O_2} further requires increasing the P_B of the slice and nutrient media together with a gas mixture containing a high fractional concentration of O_2 (F_{O_2}). Our initial find-

Address for reprint requests and other correspondence: J. B. Dean, Dept. of Physiology and Biophysics, Rm. 160 Biological Sciences Bldg., 3640 Colonel Glenn Hwy, Wright State Univ., Dayton, OH 45435 (E-mail: jay.dean@wright.edu).

[1]At sea level, P_B is 1 ATA or 760 Torr. Other commonly used pressure equivalents include 0.099 MPa (SI unit), 14.7 pounds per inch^2, and 1.01 bar.

The costs of publication of this article were defrayed in part by the payment of page charges. The article must therefore be hereby marked "*advertisement*" in accordance with 18 U.S.C. Section 1734 solely to indicate this fact.

ings, under conditions of ≤10 min of hyperbaric oxygen (HBO_2; i.e., F_{O_2} = 95–98% O_2 at P_B of 2.4–3.3 ATA), indicate a subpopulation of neurons in the solitary complex that are depolarized, exhibit increased firing rate, and, typically, have decreased membrane conductance (12, 45–46). However, these neuronal responses to HBO_2 may be blunted because slices recorded under control conditions are already hyperoxic. Moreover, we are concerned that under control conditions neuronal activity is altered by the high P_{O_2} (3, 5, 56) and increased exposure to ROS (26, 33, 54, 55). Previous electrophysiological studies in brain slices found that neuronal activity recorded in medium equilibrated with 21% O_2 is different from neuronal activity recorded in medium equilibrated with 95% O_2 (3, 5, 56). Investigators have proposed that these differences in excitability seen with 21% oxygen are not due to hypoxia, which is typically studied using 10–15% O_2 (35), but rather to normobaric hyperoxia with 95% oxygen (3, 5, 56), possibly by an increased production of ROS (26).

The goal of the present study was to measure P_{O_2} in both perfusion media and the solitary complex in slices prepared from weaned and adult rats under the same experimental conditions used in our electrophysiology studies. In doing so, we will be able to correlate changes in neuronal excitability recorded during HBO_2 with known changes in tissue P_{O_2}. Moreover, we wanted to determine the degree of hyperoxia within our brain slice model under control conditions at normobaric pressure (P_B of ~1 ATA). We hypothesize that tissue P_{O_2} will decrease in the solitary complex under control conditions (95% O_2 at P_B of ~1 ATA) with increasing tissue depth; however, tissue P_{O_2} at the center of the slice will remain hyperoxic compared with tissue P_{O_2} in the intact CNS. We also hypothesize that slice P_{O_2} will increase significantly during HBO_2. Finally, we hypothesize that tissue $\dot{V}_{O_2}$ will decrease during HBO_2 because it has previously been shown that increasing P_{O_2} of the perfusate from 150 to 600 Torr at normobaric pressure increased $\dot{V}_{O_2}$ (4), whereas HBO_2 reduced cellular $\dot{V}_{O_2}$ (1, 11). A preliminary report of these data was previously published (47).

METHODS

Pressure Terminology

The partial pressure of oxygen is the product of P_B and F_{O_2}. When varying P_B, it is important to define the P_{O_2} of the perfusate and tissue slice relative to P_B, especially when P_B and P_{O_2} are independently manipulated (12). "Normobaric pressure" refers to ambient pressure measured in our laboratory with a mercury barometer; this was slightly less than normal P_B at sea level (~1 ATA or ~760 Torr), typically ranging from 738 to 752 Torr.[2] "Hyperbaric pressure" refers to ambient pressure inside the hyperbaric chamber that is greater than 1 ATA. "Normoxia" refers to slice P_{O_2} values that approximate values measured in vivo from rats that breathed air (20–21% O_2) at normobaric pressure, i.e., CNS tissue P_{O_2} of ~10–34 Torr (Table 1). "Normobaric hyperoxia" refers to slice P_{O_2} values greater than those measured in vivo from rats breathing air at P_B ~1 ATA, i.e., >34 Torr (Table 1). Conventional brain slice control medium, including the artificial cerebral spinal fluid (aCSF) used in this study, was equilibrated with 95% O_2-5% CO_2 at normobaric pressure; thus, under control conditions, the slice was exposed to hyperoxic medium; in this study, control medium P_{O_2} values were ~708 Torr. "HBO_2" in this report describes any perfusate with P_{O_2} of >760 Torr or 1 ATA. In the present study, slices were exposed to three different HBO_2 values depending on P_B, designated here in ATA after the dash (e.g., HBO_2-2 signifies hyperoxic medium at a P_B of 2 ATA). The HBO_2 P_{O_2} values used were 1,200, 1,675, and 2,468 Torr. In this way, tissue can be exposed to hyperoxia at both normobaric pressure and hyperbaric pressure.

Brain Slices and Control Media

Slices were prepared from weaned and adult Sprague-Dawley rats as previously described (12). Anesthesia was not used because of the depressant actions these agents have on neurons (49) and their reported antagonistic interactions with elevated P_B (31, 53, 59). After decapitation, the brain stem was isolated and submerged in ice-cold (4–6°C) aCSF of the following composition (in mM): 125 NaCl, 5 KCl, 1.3 $MgSO_4$, 26 $NaHCO_3$, 1.24 KH_2PO_4, 2.4 $CaCl_2$, 10 glucose at 300 mosM, pH of ~7.45 and P_{O_2} of ~708 Torr after equilibration with a 95% O_2-5% CO_2 gas mixture at P_B of ~1 ATA. Hyperoxia (22) and HBO_2 (38, 57) both affect central respiratory control; therefore, we chose to study the effects of oxygen on a part of the brain involved in respiratory control, namely, the solitary complex. Transverse slices were cut at 300 μm starting from the obex and proceeding rostrally through the medulla oblongata. Slices were incubated in control medium at ~25°C for at least 1 h before one was selected and transferred to a tissue chamber inside the hyperbaric chamber (12). Brain slices typically remained viable for electrophysiological studies under these conditions for up to 8 h (12).

Hyperbaric Chamber

A detailed description of the hyperbaric chamber, sample cylinders, and tissue chamber are given elsewhere (13). Briefly, the hyperbaric chamber has a maximum working pressure of 65 ATA. Within the hyperbaric chamber, tissue was submerged in aCSF that was delivered at a rate of 2 ml/min using one of two high-pressure liquid chromatography (HPLC) pumps. The brain slice rested on a fine-mesh nylon grid and was stabilized by placing a large-mesh nylon grid over the top surface (Fig. 1). Temperature of the tissue bath and air above the preparation was regulated at 37 ± 0.3°C by a servo-controlled two-channel temperature controller. The tissue chamber and electronic microdrive, which was used to maneuver the P_{O_2} electrode by remote control, and various other equipment items were positioned on a retractable sled for easy access when the hyperbaric chamber was opened. Once the equipment sled was pushed in and the chamber door was sealed, the tissue slice and oxygen electrode were visualized using an externally mounted stereoscope positioned over a window in the top of the chamber. As in previous studies (12, 16, 44–48, 59), pure helium was used to hydrostatically compress the tissue bath and, hence, the brain slice. Helium is inert and of low solubility in aqueous and lipid media (2), thus helium has no partial pressure

[2] In Dayton, OH, the P_B averaged 745 ± 2 (SE) Torr. When determining medium P_{O_2}, the vapor pressure of water, which is ~48 Torr at 37 ± 0.3°C (60), was not subtracted from P_B.

Table 1. *Oxygen electrode measurements of P_{O_2} in CNS tissue, cerebrospinal fluid, and arterial blood in anesthetized rats and humans breathing air, O_2, and CO_2 gas mixtures at normobaric pressure and hyperbaric pressure*

Study	In Vivo Model	CNS Region	P_B, ATA	Inspired Gas, $\%O_2$, $\%CO_2$	Pt_{O_2}, Torr	$P_{CSF}O_2$, Torr	Pa_{O_2}, Torr
27	Adult rat, urethane	Cortex	1.0	Air	34 ± 4	33 ± 5	
			1.0	100, 0	90 ± 13	83 ± 23	
				95, 5	72 ± 12	120 ± 19	
			2.0	100, 0	244 ± 39	277 ± 50	
				95, 5	360 ± 51	402 ± 54	
			3.0	100, 0	452 ± 68	480 ± 80	
				95, 5	791 ± 51	718 ± 64	
			4.0	100, 0	643 ± 89	699 ± 106	
				95, 5	1,189 ± 195	1,053 ± 150	
			5.0	100, 0	917 ± 123	1,044 ± 131	
				95, 5	1,540 ± 94	1,540 ± 202	
			6.0	100, 0	1,293 ± 170	1,787 ± 240	
24	Adult rat, methoxyflurane	Globus pallidus	1.0	Air	11 ± 3.2		
			5.0	100, 0	620–1,250		
		Neostriatum	1.0	Air	19 ± 9		
			5.0	100, 0	490–1,010		
61	Adult rat, pentobarbital sodium	Parietal cortex	1.0	Air	12 ± 5		85 ± 4
			3.0	7, 0			150 ± 10
			3.0	100, 0			1,530 ± 24
9	Adult rat, urethane	Hypothalamus	1.0	Air	13.0 ± 3.3		
			1.0	100, 0	40.5 ± 5.9		
23	Human, anesthetized		1.0	Air		41 ± 3.4	92.7 ± 2

Values for various P_{O_2} are reported as means ± SE (either from the references given or calculated by the present authors from the data tabulated in the original article). Table 1 includes only studies that reported absolute values of P_{O_2} for central nervous system (CNS) tissue or cerebral spinal fluid (CSF). P_B, barometric pressure or ambient pressure inside room or hyperbaric chamber. One atmosphere absolute (1 ATA) is equivalent to 760 Torr (sea level). Most studies that do not use a hyperbaric chamber do not report P_B under normobaric conditions. In constructing this table, however, P_B = 1 ATA was assumed by the authors. Air refers to breathing 20–21% O_2 and balance N_2 gas mixture. The range of CNS tissue P_{O_2} (Pt_{O_2}) during hyperbaric O_2 (HBO_2) is reported in some cases because of the transient responses observed. Typically, Pt_{O_2} reached a maximum value at some point during HBO_2 and then decreased slowly. This is most likely due to regional changes in cerebral blood flow (1). Adult rat hypothalmus values are based on average calculated for 19 different nuclei in and surrounding the hypothalamus; see Table 1 in Cater et al. (9). $P_{CSF}O_2$, CSF P_{O_2}; Pa_{O_2}, arterial blood P_{O_2}.

effect [e.g., at $P_B \geq 3$ ATA, nitrogen can act as an anesthetic (31)] over the range of ambient pressures used in our study. Before compression, room air was purged from the chamber atmosphere and replaced with 100% helium; the chamber was then compressed at a rate of 2 atm/min.

Test Conditions

Equilibrating aCSF at P_B of ~1 ATA and 37°C with 95% N_2 or 95% air (balance CO_2) resulted in media with P_{O_2} values of ~0 and ~156 Torr, respectively. Hyperbaric oxygenated medium (i.e., medium that has been supersaturated with oxygen) was made by equilibrating aCSF with 98.3% O_2 at 1.6, 2.2, or 3.3 ATA in separate high-pressure sample cylinders (1-liter volume) to produce corresponding medium P_{O_2} values of ~1,200, 1,657, and 2,468 Torr. No attempt was made to keep P_{CO_2} constant at P_{O_2} of 1,200 and 1,657 Torr; however, it is possible to do so by reducing the fractional concentration of CO_2 with increased P_B (12). A pressure differential of 0.13–0.6 ATA was used to deliver hyperoxic aCSF to the tissue chamber. A high-pressure solenoid valve (General Valve, Fairfield, NJ) was used to rapidly select between control and hyperoxic medium such that perfusate flow rate was not significantly disrupted.

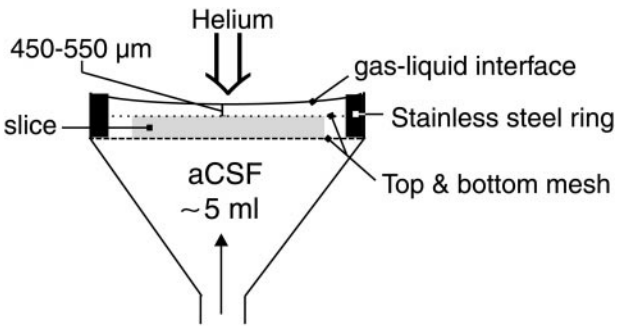

Fig. 1. Illustration of the brain slice orientation in relation to the flow of fresh oxygenated artificial cerebral spinal fluid (aCSF; not drawn to scale). Fresh aCSF enters the tissue chamber from the bottom and flows around and over the slice while a filter paper wick (not shown) draws it away from the surface.

Oxygen Measurements

Oxygen was measured using a carbon fiber needle electrode (tip outer diameter of ~10 μm), previously described by Jiang et al. (28). Electrodes were constructed by sealing an 8-μm-diameter carbon fiber (Alfa Aesar, Ward Hill, MA) at the tip of a glass pipette (MTW150–6, World Precision Instruments, Sarasota, FL) using Duco cement. The other end of the fiber was attached to a copper wire using graphite conductive adhesive (Alpha Aesar) and connected to the input of a polarographic oxygen amplifier (A-M Systems, model 1900). A −0.6-V potential was imposed between the oxygen electrode and a low-resistance (<1.0 MΩ) Ag/AgCl reference that was in contact with the tissue bath via a potassium gluconate agar bridge (12). Oxygen electrodes were typically calibrated before and after each profile in aCSF equilibrated

with 21 and 95% oxygen; only electrodes that showed a 3.5- to 4.5-fold current difference between media were used (typical slope varied between 5–10 pA/Torr).

Oxygen profiles were made by lowering the oxygen electrode in 50-μm steps perpendicular to the tissue surface. Recording depth in tissue was approximated two ways: *1*) surface depth was determined by moving the electrode down in small steps and then moving it laterally until the tip of the electrode touched the tissue, as seen by a bowing of the electrode shank during lateral movement; and *2*) core tissue depth was identified as the depth at which P_{O_2} was minimum (4, 19).

Absolute P_{O_2} values presented here were obtained directly from continual P_{O_2} recordings stored as AxoScope records (Axon Instruments, Foster City, CA) and/or on magnetic tape (Vetter PCM recorder model 400, Rebersburg, PA). Approximately one-half of the electrodes used developed drift after more than ~0.5 h in the slice, probably as the result of tissue debris on the tip (10), and resulted in an offset of 91 ± 56 Torr. If an offset developed in the measured P_{O_2}, the presented values were the sum of both the measured P_{O_2} plus any offset.

Metabolic Block Media

To minimize tissue $\dot{V}_{O_2}$, all metabolizable glucose in the aCSF was replaced with 1 mM 2-deoxy-D-glucose (2DG; Sigma Chemical, St. Louis, MO). Oxygen measurements also were made in 2DG medium supplemented with 9.1 nM antimycin A (Sigma Chemical). Antimycin A, an antibiotic that blocks electron flow from cytochrome *b* to c_1 (29), was added to the 2DG aCSF to block metabolism of substrates other then glucose (e.g., lactate).

Data Collection and Analysis

Data were collected and analyzed using a 486 PC and the AxoScope 7.0, Origin 5.0, and Mathematica software packages. Statistical significance was determined at $P < 0.05$ by one-way ANOVA and multiple comparison tests (Tukey's or Newman-Keuls) or Student's *t*-test. Linear regressions were also compared using analysis of covariance. Data are presented as means ± SE.

RESULTS

P_{O_2} Measurements in the Tissue Bath

P_{O_2} electrode calibrations. Figure 2*A* shows five superimposed P_{O_2} traces made with the oxygen electrode submerged deep into the tissue bath in the absence of a brain slice. The recordings were initiated in control aCSF with a P_{O_2} of 708 Torr. The perfusate source was

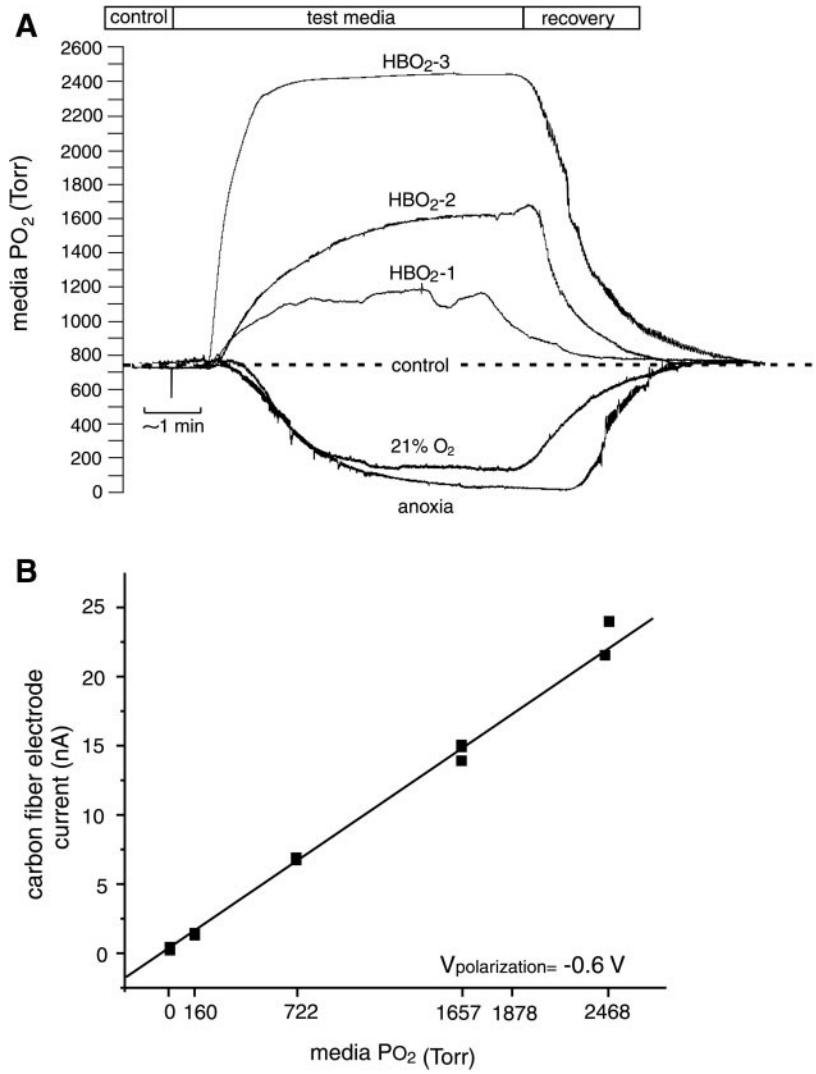

Fig. 2. *A*: continuous traces of oxygen partial pressure measured deep in the tissue bath while switching aCSF from control (P_{O_2} ~710 Torr) to aCSF with P_{O_2} values of 0, 156, 1,200, 1,657, and 2,468 Torr. All recordings were made at 37°C and at constant barometric pressure (P_B). *Bottom* 3 traces (anoxia, 21% oxygen, and HBO_2-1, where HBO_2 signifies hyperbaric O_2) were recorded at 1 atmospheres absolute (ATA), whereas the upper two traces (HBO_2-2 and HBO_2-3) were recorded while the chamber pressure was held at 2 and 3 ATA, respectively. *B*: triplicate individual current values measured during the plateau phase of each medium P_{O_2}, excluding HBO_2-1. Carbon fiber electrode produced a current that was linearly proportional to P_{O_2} from 0 to 2,468 Torr (9.6 pA/Torr, $r^2 = 0.97$, $n = 15$).

then switched to aCSF with P_{O_2} values of 0, 156, 1,200, 1,657, and 2,468 Torr to produce normobaric anoxia, 21% oxygen, HBO_2-1 (P_B of 1 ATA), HBO_2-2 (P_B of 2 ATA), and HBO_2-3 (P_B of 3 ATA), respectively. During HBO_2-1, P_{O_2} recordings were less stable because, as the pressure differential between the medium and tissue chamber approached 2:1, small oxygen bubbles would form in the aCSF inflow line and tissue bath, which disrupted the perfusate flow rate and aCSF meniscus in the tissue chamber. When the control medium was switched to one of the test media, a short delay in the electrode response was observed due to the dead space between the medium reservoirs and tissue chamber. Figure 2*B* shows that the polarographic electrode current measured at the plateau phase of each curve in Fig. 2*A* was linearly proportional to medium P_{O_2} at both normobaric and hyperbaric pressure over a range of P_{O_2} values from 0 to 2,468 Torr.

Gas-liquid oxygen diffusion gradient. At an interface between gas and liquid media with dissimilar oxygen tensions, oxygen will diffuse down its chemical gradient. In our submerged slice preparation, oxygenated aCSF was in contact with an anoxic gaseous atmosphere (100% helium). Consequently, P_{O_2} was measured as a function of aCSF depth into the tissue bath to determine the extent to which medium P_{O_2} dropped as a result of diffusion into the chamber atmosphere. The P_{O_2} measurements shown in Fig. 3 were made in the tissue bath without a brain slice present. The recordings were initiated at the tissue bath surface in aCSF, with P_{O_2} values of ~708, 1,657, or 2,468 Torr. The electrode was then moved through the aCSF in 50-μm steps until the recorded P_{O_2} reached a stable plateau. These measurements show that bath P_{O_2} increased at depths into medium between 0 and ~450 μm, thus signifying the presence of an oxygen diffusion layer that was probably due to a loss of oxygen from the aCSF to the chamber atmosphere. The relative oxygen gradient, expressed as a percentage of the maximum P_{O_2} at 450 μm, at each medium P_{O_2}, was similar. For instance, the steady-state P_{O_2} at depths of 100, 250, or 450 μm, were ~20, 50, or 100%, respectively, of the maximum P_{O_2}. The independence of the relative oxygen diffusion gradient from medium P_{O_2} may result from the configuration of our perfusion system. Fresh oxygenated aCSF is delivered to the tissue chamber from the bottom where it flows up toward the surface. We assumed that P_{O_2} of the chamber atmosphere remained negligible since the hyperbaric chamber volume was considerably larger (72 liters) than the tissue chamber volume (~ 5 ml) and the frequent flushing of the hyperbaric chamber atmosphere with fresh helium gas further minimized any P_{O_2} buildup.

P_{O_2} Measurements in the Slice

Regular aCSF. A total of 38 P_{O_2} profiles were made in 300-μm-thick brain slices perfused with aCSF having P_{O_2} values that ranged from 156 to 2,468 Torr. Examples of individual profiles made at 708, 1,657, and 2,468 Torr are shown in Fig. 4. The brain slice was positioned ≥500 μm from the gas-liquid interface. The recordings began while the electrode was positioned 200 μm above the tissue surface. Although the distance of the initial recording position from the surface of the bath was not measured directly, it was estimated to be 250–350 μm, based on the gas-liquid oxygen diffusion gradient (Fig. 3), assuming that the slice does not

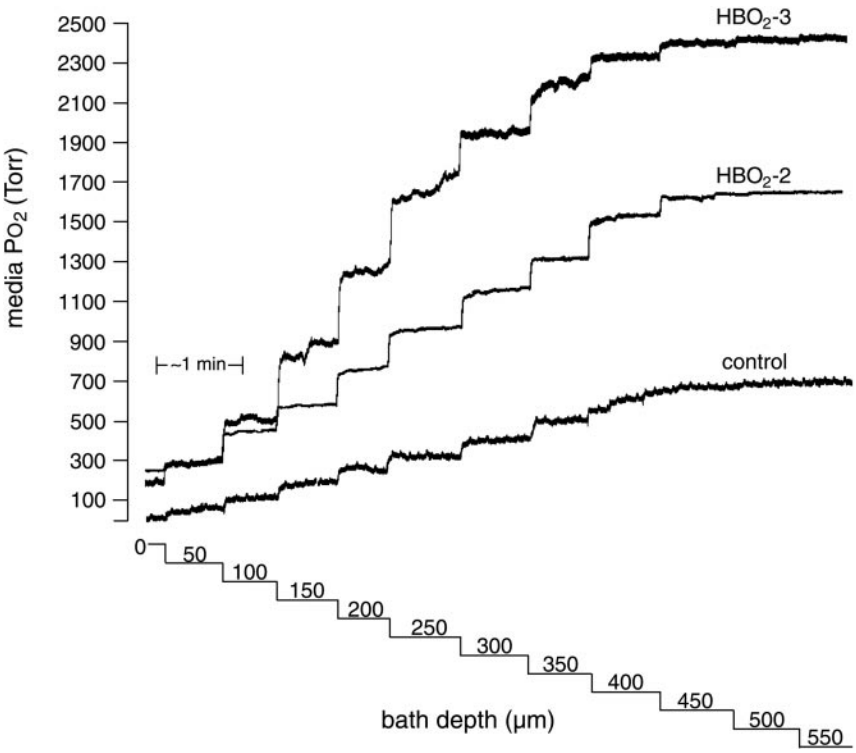

Fig. 3. An oxygen diffusion gradient was measured under control and hyperoxic conditions in the absence of a brain slice. Oxygen measurements were initiated while the oxygen electrode was positioned at the surface of the aCSF. Then, moving in 50-μm increments, the electrode was driven into the aCSF, which flowed into the ~5-ml chamber at a rate of 2 ml/min. Medium P_{O_2} was lowest at the interface where O_2 diffused into the gas phase of the overlying atmosphere. Medium P_{O_2} increased with depth reaching a maximum value at a depth of ~450 μm for each medium. The results were similar for 2 additional trials using HBO_2.

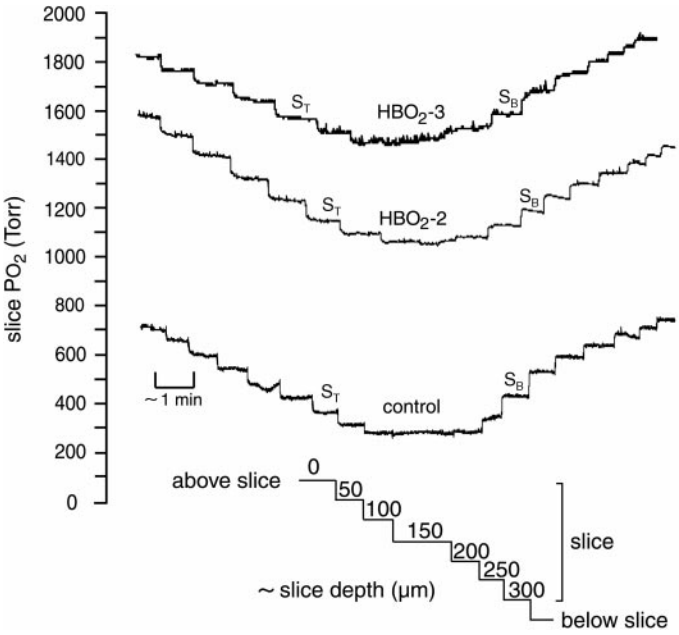

Fig. 4. Continual P_{O_2} measurements were made through 300-μm-thick brain slices equilibrated with control (P_{O_2} ~ 708 Torr) or hyperoxic (HBO_2-2 and HBO_2-3) aCSF. For the *top* 2 traces, the perfusate was switched to hyperoxic medium and allowed to establish a new stable P_{O_2} before the electrode was moved toward the tissue in 50-μm steps. Profiles were initiated 200 μm above the surface of slice. The designation "S_T" signifies when the electrode was closest to the top surface of the slice; "S_B" signifies when the electrode was closest to the slice bottom. With each step, the corresponding change in P_{O_2} was allowed ~1 min to stabilize before the next step. The depth scale under the P_{O_2} traces corresponds to the control P_{O_2} profile. Notice that P_{O_2} declined above the slice and increased below the slice, thus indicating the presence of a diffusion layer at each surface of the slice.

influence oxygen diffusion into the chamber atmosphere. In contrast to Fig. 3, P_{O_2} decreased in the aCSF as the oxygen electrode moved deeper into the bath toward the surface of the submerged tissue slice in Fig. 4, undoubtedly due to $\dot{V}_{O_2}$ by the slice. Once the oxygen electrode was in the slice, P_{O_2} decreased further to a minimum at the slice core (~150 μm), after which tissue P_{O_2} increased as the oxygen electrode approached the lower surface of the slice. Likewise, P_{O_2} in the bath increased as the electrode moved away from the lower surface of the slice. This indicated that an oxygen diffusion layer in the aCSF (~200 μm thick) was present around each surface of the tissue, with a magnitude roughly equivalent to the oxygen diffusion gradient in the first 100 μm of tissue. Figure 5 summarizes the dynamics of oxygen diffusion in our submerged slice preparation and further illustrates the significant effect that these oxygen diffusion gradients have on setting P_{O_2} in the aCSF and slice.

Tissue P_{O_2} measured at the surface (0 μm) of the slice and at a maximum depth of 150 μm were averaged to estimate mean tissue P_{O_2} and plotted against medium P_{O_2} in Fig. 6. Table 2 summarizes mean tissue P_{O_2} plotted in Fig. 6 as well as values measured at a depth of 50 and 100 μm into tissue. Increasing P_{O_2} of the medium from 156 to 2,468 Torr increased tissue P_{O_2} measured at 0 and 150 μm depths proportionally; slopes of regression lines were 0.65 ± 0.02 (r^2 = 0.998, n = 38) and 0.66 ± 0.04 (r^2 = 0.997, n = 38) at the surface and core, respectively. However, mean tissue P_{O_2} measured at 0 and 150 μm were significantly different at medium P_{O_2} values of 156, 708, and 1,200 Torr. As medium P_{O_2} increased beyond 1,200 Torr, there was no statistical difference in mean P_{O_2} measured at the tissue surface and tissue core. These results suggest slice $\dot{V}_{O_2}$ may have decreased during exposure to the higher levels of HBO_2 (see *Metabolically Poisoned Tissue* below).

In our electrophysiological studies of how HBO_2 affects neuronal excitability (12, 45, 46), it was important to differentiate the effects of pressure per se (i.e., hyperbaric helium) from those of high P_{O_2}; thus tissue P_{O_2} measurements were made in tissue equilibrated with a constant control level of P_{O_2} (~708 Torr) at P_B of 1, 2, and 3 ATA. The hyperbaric chamber was compressed with 100% helium and allowed 2–5 min for equilibration before tissue P_{O_2} was measured at a depth of 150 μm. Results from these measurements are plotted in Fig. 6. Tissue P_{O_2} at 2 and 3 ATA were not significantly different from P_{O_2} measured at 1 ATA, and the slope of the regression line, 0.04 ± 0.04 (r^2 = 0.772, n = 3), was not significantly different from zero. These results indicate that the effect of pressure per se can be differentiated from increased oxygen tension. It also indicates that 2 and 3 ATA of pressure do not affect oxygen diffusion or utilization (12, 47).

Metabolically poisoned tissue. A series of P_{O_2} profiles were made in slices incubated at medium P_{O_2} values ranging from 156 to 2,468 Torr in 2DG aCSF or 2DG plus antimycin A. This was done to determine how $\dot{V}_{O_2}$ affects slice P_{O_2} (i.e., the magnitude of P_{O_2} profiles between the slice surface and the core of the slice). The difference in P_{O_2} measured at the slice surface (0 μm) to its core (150 μm) was defined as delta P_{O_2} (ΔP_{O_2}). By comparing the ΔP_{O_2} measured in metabolically active slices at different medium P_{O_2} values with the same measurements made in metabolically poisoned slices, the P_{O_2} dependence of $\dot{V}_{O_2}$ could be determined. Mean slice P_{O_2} measured at 150 μm in slices perfused with 2DG and 2DG plus antimycin A medium was linearly related to medium P_{O_2}. No significant difference existed between the slopes of regression lines for each data set; therefore, the 2DG data and antimycin A supplemented 2DG data were pooled. The slope of pooled data vs. medium P_{O_2} was 0.74 ± 0.03 (r^2 = 0.997, n = 33).

Figure 7*A* shows superimposed P_{O_2} profiles, measured at 708 Torr, in regular and a metabolically poisoned brain slice. For comparison, mean P_{O_2} values measured at depths of 0, 50, 100, and 150 μm in metabolically poisoned slices are given in Table 2. In this example, ΔP_{O_2} was smaller in metabolically poisoned tissue (ΔP_{O_2} = 66 Torr) compared with metabolically active tissue (ΔP_{O_2} = 116 Torr). We considered the difference in ΔP_{O_2} between metabolically active tissue and 2DG tissue to be proportional to $\dot{V}_{O_2}$. Consequently, ΔP_{O_2} in nonpoisoned tissue was used as an

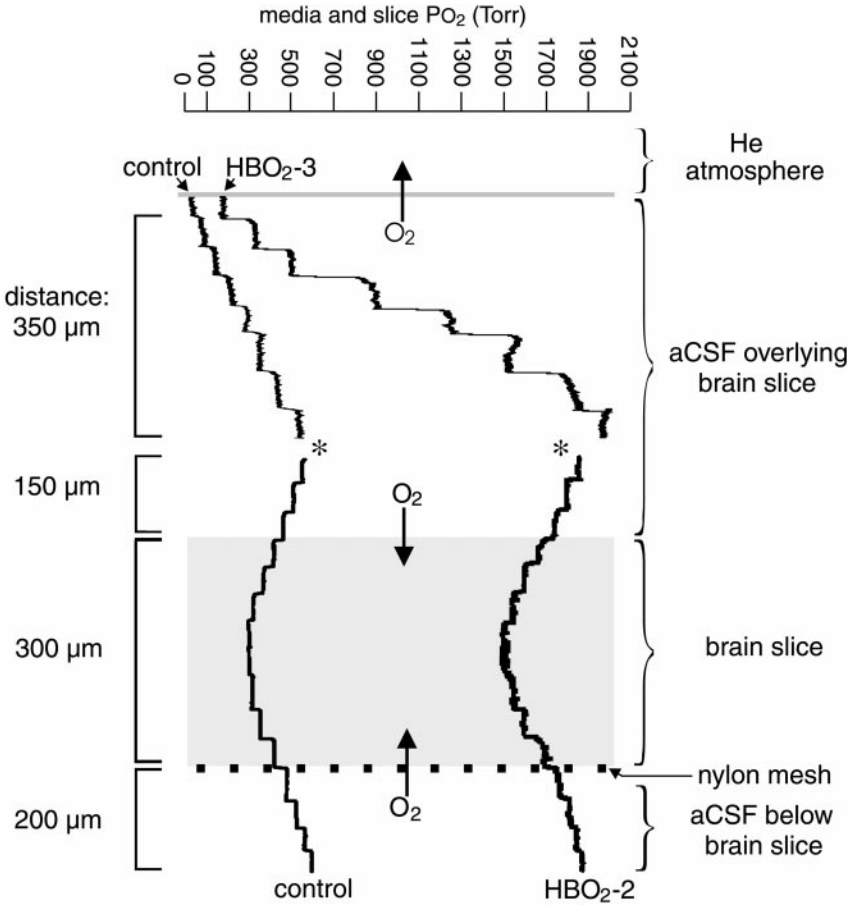

Fig. 5. P_{O_2} traces were plotted as a function of aCSF and slice depth. Traces of P_{O_2} made during control (708 Torr) and HBO_2-3 (2,468 Torr) conditions show bath P_{O_2} increasing with distance (50-μm steps) from the aCSF meniscus. As the electrode approached the surface of the slice, P_{O_2} began decreasing. *Not a continuous recording. Arrows at the He gas-aCSF and slice-aCSF interfaces indicate the direction of oxygen diffusion. Measured P_{O_2} reached a relative minimum at the slice core, after which P_{O_2} increased as the electrode passed through and away from the bottom of the brain slice. Typically, P_{O_2} recordings were terminated ~200 μm past the bottom of the slice.

indirect measure of $\dot{V}_{O_2}$ to gain insight as to how HBO_2 affects $\dot{V}_{O_2}$. Mean ΔP_{O_2} values were measured in metabolically active and inactive tissue and plotted against medium P_{O_2} in Fig. 7*B*. Mean ΔP_{O_2} values measured in metabolically poisoned slices did not vary significantly over the entire range of medium P_{O_2} values studied. This indicated that the effects of P_{O_2} on nonmetabolic forms of oxygen utilization (e.g., formation of ROS) were negligi-

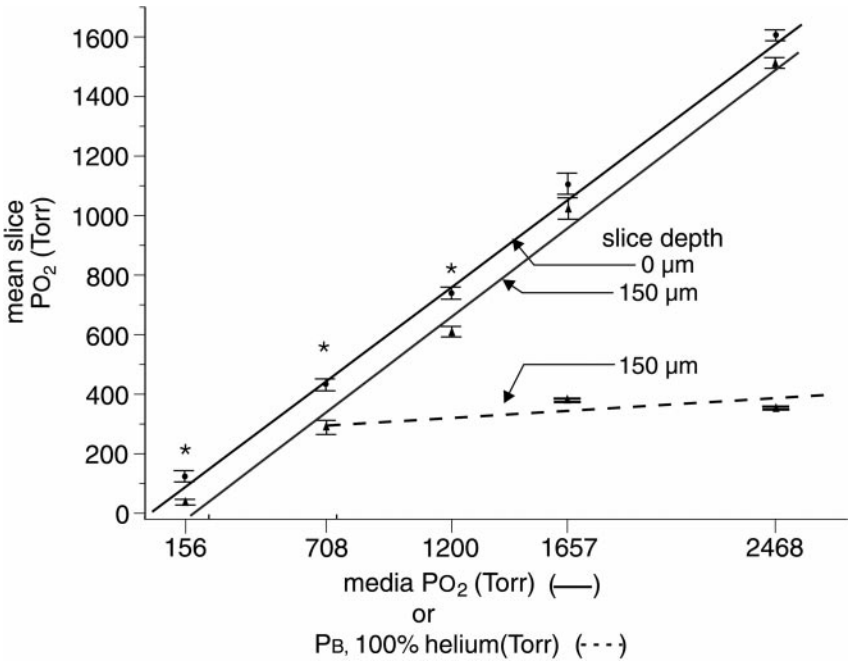

Fig. 6. Mean P_{O_2} (n = 3–13, see Table 1) measured in regular aCSF at the slice surface (0 μm) and at the center of the slice (150 μm) were plotted against media P_{O_2}. Oxygen tension measured at 0 μm differed significantly (*$P < 0.05$) from values measured at 150 μm at $P_{O_2} \leq 1{,}200$ Torr. At a constant P_{O_2} of ~708 Torr, slice P_{O_2} at 150 μm was measured in slices compressed with helium to P_B of 1, 2, and 3 ATA, and these mean P_{O_2} values (n = 3) were plotted as the dashed line. At ~708 Torr, P_{O_2} measured at 2 and 3 ATA were not significantly different from P_{O_2} measured at 1 ATA.

Table 2. *Mean tissue P_{O_2} in regular aCSF and in aCSF with 2DG and antimycin A*

Tissue Depth	P_{O_2} of Medium, Torr				
	156	708	1,200	1,657	2,468
			Regular aCSF		
Surface	136 ± 17(3)	436 ± 21(13)	742 ± 21(3)	1,105 ± 40(8)	1,613 ± 16(6)
50 μm	79 ± 9(6)	368 ± 22(13)	700 ± 10(5)	1,058 ± 39(8)	1,570 ± 11(6)
100 μm	52 ± 9(4)	319 ± 24(13)	665 ± 18(5)	1,036 ± 41(8)	1,537 ± 13(6)
150 μm	40 ± 7*(6)	291 ± 20*(13)	616 ± 16*(5)	1,021 ± 40(8)	1,517 ± 15(6)
			2DG + antimycin A aCSF		
Surface	117 ± 5(3)	607 ± 14(8)	955 ± 17(3)	1,207 ± 53(9)	1,828 ± 106(7)
50 μm	77 ± 12(6)	573 ± 16(8)	924 ± 22(3)	1,177 ± 53(9)	1,808 ± 107(7)
100 μm	49 ± 9(6)	550 ± 21(8)	893 ± 16(3)	1,158 ± 54(9)	1,783 ± 109(7)
150 μm	25 ± 9(6)	532 ± 23†(8)	876 ± 20†(3)	1,115 ± 47(11)	1,773 ± 107(7)

Values are means ± SE; *n* (in parentheses) = no. of slices. 2DG, 2-deoxy-D-glucose. *$P < 0.05$, surface Pt_{O_2} at 0 μm is greater than core Pt_{O_2} at 150 μm; †$P < 0.05$; core Pt_{O_2} at 150 μm is greater in 2DG-antimycin A aCSF than core Pt_{O_2} at 150 μm in regular aCSF.

ble in this comparison. However, ΔP_{O_2} measured in metabolically active slices at 708 Torr was significantly greater than ΔP_{O_2} measured in metabolically poisoned slices; however, as medium P_{O_2} increased from 708 to 2,468 Torr, ΔP_{O_2} values measured in metabolically active slices got smaller and more closely resembled profiles in metabolically poisoned slices, thus suggesting $\dot{V}_{O_2}$ was reduced during exposure to HBO_2.

The oxygen diffusion coefficient (D) and $\dot{V}_{O_2}$ were calculated to better describe the dynamics of oxygen in our preparation over a broad range of P_{O_2} values as well as to quantify, if only by approximation, the relationship between $\dot{V}_{O_2}$ and tissue P_{O_2} (see APPENDIX for details regarding the calculations of D and $\dot{V}_{O_2}$). During measurements of oxygen at a constant depth of 150 μm in a metabolically poisoned brain slice, D was determined by measuring the change in P_{O_2} over time when switching between two media with different nonzero P_{O_2} values (8, 17), in this case 708 and 156 Torr. With the assumption that all forms of oxygen utilization were constant, D was estimated to be 1.3×10^{-6} cm^2/s. Our estimated D was smaller by about one-tenth than the D calculated from P_{O_2} measurements in 1,000-μm-thick slices of cat cortex equilibrated with a similar initial P_{O_2}, 1.54×10^{-5} cm^2/s (21).

$\dot{V}_{O_2}$ rate can be calculated from tissue oxygen profiles using Fick's second law of diffusion (20). With the use of boundary conditions of P_{O_2} at the surface of the slice (defined as P_0) and at the bottom of the slice [defined as P_L; thickness of the slice (L) = 300 μm], our slice P_{O_2} profiles at each medium P_{O_2} were fitted to the parabolic equation (20)

$$P_{O_2} = aX^2 - \left(aL + \frac{P_0 - P_L}{L}\right)x + P_0$$

where P_{O_2} is oxygen tension measured at depth X in a brain slice, $a = \dot{V}_{O_2}/2DS$, and S is the estimated solubility coefficient of oxygen in cat brain (1.89×10^{-5} ml $O_2 \cdot cm^{-3} \cdot Torr^{-1}$) (21). Using our estimated D (1.3×10^{-6} cm^2/s), we calculated the $\dot{V}_{O_2}$ (mean ± SE ml $O_2 \cdot cm^{-3} \cdot min^{-1}$) at each medium P_{O_2} to be $1.4 \pm 0.17 \times 10^{-3}$ at 156 Torr, $1.8 \pm 0.2 \times 10^{-3}$ at 708 Torr, $1.9 \pm 0.32 \times 10^{-3}$ at 1,200 Torr, $1.7 \pm 0.75 \times 10^{-3}$ at 1,657 Torr, and $9.3 \pm 1.3 \times 10^{-4}$ at 2,468 Torr. Although $\dot{V}_{O_2}$ at 1,200 and 1,657 Torr were not less than $\dot{V}_{O_2}$ at 708 Torr (i.e., $\dot{V}_{O_2}$ and ΔP_{O_2} were not well matched), a trend of decreasing $\dot{V}_{O_2}$ was evident at 2,468 Torr. These results suggest $\dot{V}_{O_2}$ was dependent on P_{O_2} during hyperoxia; therefore, we incorporated this assumption into our calculation of $\dot{V}_{O_2}$ (see APPENDIX) and estimated $\dot{V}_{O_2}$ at a constant depth by measuring the rate of change in P_{O_2} measured in a metabolically active slice exposed to different aCSF P_{O_2} values (8). Oxygen measurements were made at a constant depth of 150 μm in a brain slice while media P_{O_2} changed from ~708 to ~156 Torr or from ~708 to ~2,468 Torr. From these measurements, we estimated $\dot{V}_{O_2}$ to be 7.9×10^{-5} and 7.3×10^{-6} ml $O_2 \cdot cm^{-3} \cdot min^{-1}$, respectively. Although the absolute values varied, both methods of determining $\dot{V}_{O_2}$ showed that $\dot{V}_{O_2}$ was consistently reduced under the more extreme hyperoxic conditions compared with control P_{O_2} values.

DISCUSSION

Neuronal tissue P_{O_2} has been measured in the intact CNS during HBO_2 (24, 27, 51, 61), and in brain slices at normobaric pressure (3–5, 19–21, 28, 50, 56); however, this is the first study to systematically study P_{O_2} gradients in brain slices during HBO_2. We found that, under conventional brain slice control conditions (95% O_2), P_{O_2} measured in the solitary complex decreased with increasing recording depth to a minimum P_{O_2} value at the core of the slice that was still ~10-fold higher than normal cerebral P_{O_2} in vivo, which has been reported to range from 10 to 34 Torr (Table 1). In fact, at an aCSF P_{O_2} of 708 Torr, P_{O_2} at the core of the slice approximated P_{O_2} measured in the CNS of rats breathing 100% oxygen at P_B of >2 ATA (27). Furthermore, tissue P_{O_2} increased linearly with aCSF P_{O_2} from 156 to 2,468 Torr, to levels that are known to result in CNS O_2 toxicity in whole animals (1, 25, 58). This range of HBO_2 has been reported to depolarize solitary complex neurons in brain stem slices after ≤10 min of exposure (12, 45, 46). At P_{O_2} values >1,200 Torr, the

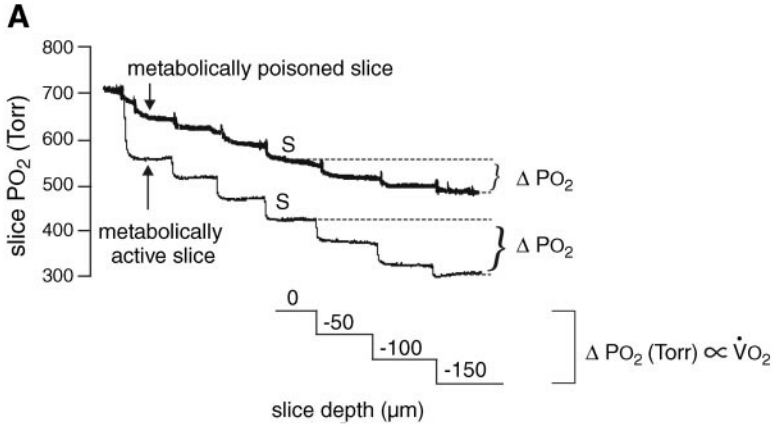

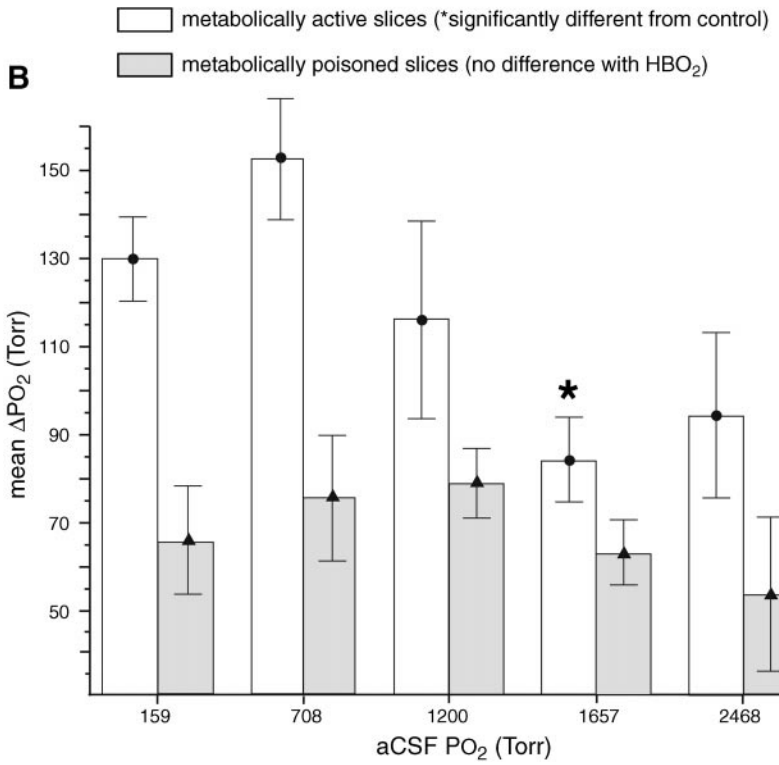

Fig. 7. *A*: 2 superimposed P_{O_2} profiles measured at ~708 Torr in a metabolically active and metabolically inactive slice. The difference in P_{O_2} from the slice surface (0 μm) to its core (150 μm) was defined as delta (Δ) P_{O_2}. *B*: ΔP_{O_2} measured in metabolically active tissue at a P_{O_2} of ~708 Torr was significantly greater ($P < 0.05$) than ΔP_{O_2} in metabolically poisoned tissue at all P_{O_2} tested. During HBO_2, the ΔP_{O_2} values measured in metabolically active brain slices were reduced to values that more closely resembled ΔP_{O_2} in metabolically poisoned slices. *P_{O_2} measured in metabolically active slices at which the ΔP_{O_2} was significantly ($P < 0.05$) smaller than ΔP_{O_2} measured at ~708 Torr. These results suggest that oxygen consumption is reduced by HBO_2.

difference in P_{O_2} from the surface to tissue core (i.e., ΔP_{O_2}) decreased to the extent that ΔP_{O_2} measured in metabolically active tissue exposed to hyperoxic medium no longer differed from ΔP_{O_2} made in metabolically poisoned tissue. This difference was attributed to a reduction in $\dot{V}_{O_2}$, suggesting that the higher levels of HBO_2 may decrease cellular respiration in brain slices, as previously reported (1, 11).

Critique of Methods

Initially, we measured oxygen with platinum needle electrodes (12); however, these electrodes showed poor resolution between 50-μm steps in tissue (not shown). This resolution problem likely resulted from the high rate of $\dot{V}_{O_2}$ by the electrode, as signified by the large current generated per Torr oxygen (7.87 nA/Torr), which then depleted oxygen from the area around the electrode tip, thus blunting the P_{O_2} difference per 50 μm. Therefore, we switched to carbon fiber electrodes of the type typically used for the voltametric detection of neurotransmitters and metabolites around synapses (41). Polarographic electrodes can measure oxygen at a polarization potential of −0.6 V with minimal interference from oxidizable substances (e.g., neurotransmitters are typically oxidized at potentials of 0.2–0.8 V), and, because these electrodes are small and of high resistance, they are ideal for measuring oxygen in brain slices (28). Only carbon fiber electrodes were used in this study; as illustrated in Fig. 2B, these electrodes produced a current that was linearly proportional to oxygen concentration at both normobaric and hyperbaric pressure.

As was the case in previous studies (4, 19, 21), there was considerable variability in our P_{O_2} measurements. This variability likely resulted from error in the estimated tissue depth due to tissue dimpling as the electrode penetrated the slice, uneven brain slice thickness, or tissue debris on the electrode tip that reduced the tip surface available for the reduction of oxygen (10). Likewise, tissue debris on the electrode tip likely accounted for offsets that occurred in about one-half of the electrodes used. Slow tissue potential changes or direct current shifts, which can influence P_{O_2} measurements,[3] were presumed to be small in the solitary complex during exposure to the same hyperoxic conditions, compared with the −0.6-V polarizing potential (12, 45, 46). Furthermore, it has also been shown that, when using a low-resistance remote reference, the effects of any slow tissue potential changes on the polarizing voltage were negligible (37). More stable methods of measuring P_{O_2}, such as with a Clark-style oxygen electrode (17) or the optical phosphorescence method (32), were not used because of the constraints of doing such measurements inside a hyperbaric chamber at P_B >1 ATA.

P_{O_2} Profiles in aCSF

At the gas-liquid interface, oxygenated aCSF was in contact with an oxygen-free helium atmosphere. Oxygen, according to Le Châtelier's principle, will diffuse from the aCSF down its chemical gradient into the overlying chamber atmosphere, leaving behind a graded layer of P_{O_2} in the aCSF. As expected, P_{O_2} was minimum at the aCSF surface and increased with increasing depth of aCSF. However, the depth at which a measurable diffusional loss of oxygen to the chamber atmosphere no longer occurred was consistently ~450 μm regardless of the media P_{O_2}. In addition, our results indicate that submerged brain slices are oxygenated by the diffusion of oxygen from aCSF of approximately ±200 μm to the tissue surface. We observed that, at medium P_{O_2} values ≥708 Torr, oxygen diffusion into the brain slice resulted in a 35–40% drop in P_{O_2} from bulk aCSF to slice surface. Previous studies have noted similar diffusion layers, sometimes referred to as unstirred layers in brain slices (4, 19, 21, 39) and in the brain stem spinal cord preparation (52).

If we assume that the oxygen diffusion gradient in the bath is identical with or without the tissue slice present, then these results suggest that oxygenation of the top surface of the slice is limited by the following two factors: *1*) the diffusion of oxygen into the helium atmosphere and *2*) the depth of the aCSF overlying the slice. Thus maintaining <450 μm of perfusate over the slice could potentially limit oxygenation at the upper surface of the slice. In our preparation, however, the brain slice was always positioned >450 μm deep to the bath surface.

P_{O_2} Profiles in Brain Slices

Measurements of P_{O_2} through 300-μm-thick brain slices exposed to medium P_{O_2} ranging from 156 to 2,468 Torr showed that, although oxygen tension decreased with increasing recording depth in tissue, P_{O_2} measured at the tissue surface (0 μm) and tissue core (150 μm) increased linearly as medium P_{O_2} increased. As expected, these results indicate that the oxygen diffusion coefficient in tissue did not change with medium P_{O_2} or diffusion distance. Furthermore, the magnitude of the oxygen gradient in aCSF from ≤200 μm above or below the slice was roughly equivalent to the oxygen gradient in the outer 100-μm layers of tissue. A similar observation was previously reported in the neonatal rat brain stem spinal cord preparation (52).

The majority of our tissue P_{O_2} profiles were symmetrical, with the minimum P_{O_2} value measured approximately at the center of the slice. Some studies conducted at normobaric pressure came to similar conclusions (19–21). In contrast, investigators who used the interface slice preparation, with an overlying atmosphere of 95% O_2, reported that diffusion from the upper surface dominated and resulted in a minimum P_{O_2} near the bottom of the slice (28).

Control P_{O_2} at Normobaric Pressure

When slices were submerged in aCSF equilibrated with 95% O_2, we measured a minimum P_{O_2} of 291 ± 83 Torr at the center of the slice. A similar minimum P_{O_2} value of 187.2 ± 11 Torr (n = 2) was measured at a depth of 150 μm in 320-μm-thick guinea pig cortical slices submerged in aCSF equilibrated with 95% O_2 at 1 ATA (19). Likewise, although variability between brain slice preparations and experimental parameters makes direct comparison of absolute slice P_{O_2} difficult, minimum control P_{O_2} values reported here were similar to values measured in 400- to 450-μm thick brain slices positioned in the interface preparation; these values ranged from ~150 to 280 Torr (28, 50).

Minimum P_{O_2} values measured in our slice preparation and in others (19, 28, 50) when incubated with conventional control solution (95% O_2, P_B of 1 ATA) were ~10-fold greater than P_{O_2} values measured in vivo (9, 23, 24, 27, 51, 61). This indicates that most brain slice studies are performed under hyperoxic conditions at normobaric pressure, thus raising the concern that neuronal activity may be affected by an increased production of ROS. It has been shown that the degree of tissue damage resulting from lipid peroxidation was significantly increased in brain slices incubated in 95% O_2 compared with 21% O_2 at normobaric pressure (33, 54). Bingmann and colleagues (3, 5) found neurons in hippocampal slices incubated in ~21% O_2 depolarized and increased their firing rate when exposed to 100% O_2, indicating that the high P_{O_2}

[3]Lehmenkuhler et al. (37) reported that, when making P_{O_2} measurements in excitable tissue, slow tissue potential changes or direct current shifts resulting from oxygen-induced excitation may mimic changes in P_{O_2} by interfering with the polarizing voltage at the oxygen electrode.

of brain slice control medium (i.e., normobaric hyperoxia) can, in fact, alter cellular activity. The activity of hippocampal neurons in 21% O_2 was not considered a response to hypoxia (in the brain slice preparation, hypoxia is typically mimicked by Fo_2 values of 10–15% O_2 at P_B of 1 ATA), however, because the activity of hippocampal neurons exposed to hypoxia was quite different (15, 36). Normobaric hyperoxia has also been shown to alter neuronal function in hypothalamic slices (55) and in the carotid body (43), and these responses were attributed to increased ROS.

Characterization of an optimal medium P_{O_2} has proven to be important for thin tissue preparations like neuronal cell cultures. For example, in cultures of neocortical and hippocampal neurons, the optimal medium P_{O_2}, based on cell growth and viability, was determined to be 9% O_2 at P_B of 1 ATA (~68 Torr) (7, 30). Neuritogenesis of cultured hippocampal neurons was also improved by the addition of antioxidants (vitamin E, vitamin A, and linolenate) to the incubation medium (7). These results suggest that the optimal medium P_{O_2} for an in vitro tissue preparation must balance tissue oxygen requirements with the otherwise toxic oxidative effects of excess oxygen.

Clearly, medium P_{O_2} affects both neuronal viability and excitability. For this reason, it is important that in vitro experimental conditions match, as closely as possible, in vivo conditions (i.e., optimum Fo_2 of the perfusion medium should produce a P_{O_2} at the core of the brain slice that ranges between 10 and 34 Torr). In our study, when medium P_{O_2} was reduced from control to 21% O_2, although slice surface P_{O_2} was still hyperoxic, the minimum P_{O_2} values, which averaged 40 ± 17 Torr, more closely resembled P_{O_2} values measured in the CNS and CSF of whole animals (Table 1). Alternatively, antioxidants can be added to the medium to provide protection from ROS when using 95% O_2 (6, 7, 34). Subsequent electrophysiological studies of solitary complex neurons in 300-μm-thick brain slices are required to confirm, however, that cells remain viable and healthy in this preparation at this lower level of control P_{O_2}.

Metabolically Poisoned Tissue

$\dot{V}_{O_2}$ is another important factor that must be considered when determining the optimum brain slice control P_{O_2}. Bingmann et al. (4) reported that cellular $\dot{V}_{O_2}$ increased when the incubation medium P_{O_2} of 300-μm-thick hippocampal slices increased from 150 to 600 Torr. The authors suggested that, at normobaric pressure and a medium P_{O_2} of 150 Torr, cell respiration was limited by oxygen availability such that an increase in medium P_{O_2} resulted in an increase in $\dot{V}_{O_2}$. However, the extent to which brain slice $\dot{V}_{O_2}$ is directly dependent on medium P_{O_2} is not known under conditions of HBO_2. For these reasons, we measured P_{O_2} in brain slices equilibrated with aCSF having P_{O_2} values that ranged from 156 to 2,468 Torr; then, for comparison, P_{O_2} measurements were repeated in metabolically poisoned tissue equilibrated with the same range of P_{O_2} values. Oxygen profiles in metabolically active slices showed that, as P_{O_2} increased from 708 to 1,657 Torr, the ΔP_{O_2} approached a minimum, at 1,657 Torr, that was significantly different from the ΔP_{O_2} at 708 Torr and not different from ΔP_{O_2} values in metabolically poisoned tissue. At P_{O_2} greater than 1,657 Torr, ΔP_{O_2} values of oxygen profiles remained similar in magnitude to ΔP_{O_2} values made in metabolically poisoned tissue. In addition, calculated $\dot{V}_{O_2}$ under control conditions (95% O_2) was $1.8 \pm 0.2 \times 10^{-3}$ ml $O_2 \cdot cm^{-3} \cdot min^{-1}$. A comparable $\dot{V}_{O_2}$ of $3.38 \pm 0.31 \times 10^{-2}$ ml $O_2 \cdot cm^{-3} \cdot min^{-1}$ was measured in 500-μm-thick slices of guinea pig olfactory cortex equilibrated with 95% O_2 (20). During HBO_2-3, $\dot{V}_{O_2}$ was reduced to $9.3 \pm 1.3 \times 10^{-4}$ ml $O_2 \cdot cm^{-3} \cdot min^{-1}$. Furthermore, although absolute $\dot{V}_{O_2}$ values varied, this trend was maintained when $\dot{V}_{O_2}$ was assumed to be dependent on medium P_{O_2} (see APPENDIX). Together, these results suggest that the higher levels of HBO_2 reduced metabolism in 300-μm-thick slices.

The mechanism by which HBO_2 may reduce brain slice metabolism is not clear but likely involves the increased production of ROS and the oxidation of mitochondrial enzymes and/or cofactors, including α-lipoic acid, cytochrome *c*, flavin nucleotides, and ubiquinone (1, 11). Furthermore, neuronal responses to HBO_2 depend on the duration of the HBO_2 exposure. Previous electrophysiological recordings show that short (≤10 min) bouts of HBO_2 increase neuronal activity (12, 45, 46); it is well known that $\dot{V}_{O_2}$ increases in conjunction with neuronal activity (42); however, in this study, we presented evidence suggesting that 30 min or more of exposure to the same HBO_2 actually reduced $\dot{V}_{O_2}$. Future studies focusing on the details regarding the dose dependence of HBO_2 sensitivity may be necessary.

In conclusion, oxygen tension in the submerged brain slice during normobaric hyperoxia and HBO_2 was a complex function that was dependent on several experimental conditions, including ambient P_{O_2}, depth of slice in the tissue bath, and $\dot{V}_{O_2}$. Our findings show that P_{O_2} in the solitary complex of the 300-μm-thick brain slice submerged in control medium (95% O_2 at P_B of ~1 ATA) was hyperoxic compared with the in vivo CNS. When exposed to HBO_2, tissue P_{O_2} increased to oxygen tensions that corresponded with cerebral P_{O_2} values measured in vivo under conditions that result in symptoms of CNS O_2 toxicity (1, 25, 58). Our results also suggest that metabolism decreased during high levels of HBO_2, which was consistent with previous observations (1, 11) and suggests that there may be a metabolic component to the mechanism of HBO_2-induced neuronal sensitivity.

APPENDIX

By assuming one-dimensional diffusion and uniform boundary conditions across the surface of the slice, *D* can be

approximated by the solution to Fick's second law of diffusion (8)

$$P_{O_2} \approx P_1 + \frac{4(P_0 - P_1)}{\pi} \sin\left(\frac{\pi X}{L}\right) \exp\left[-D\left(\frac{\pi}{L}\right)^2 t\right]$$

where P_0 is the measured P_{O_2} at a depth of 150 μm in tissue equilibrated with a medium P_{O_2} of 708 Torr, P_1 is the measured P_{O_2} at a depth of 150 μm in tissue equilibrated with a medium P_{O_2} of 156 Torr, P_{O_2} is calculated to be the mean of P_0 and P_1, X is the recording depth (150 μm), L is tissue thickness (300 μm), and t is time, in seconds, to reach P_{O_2}. We calculated D at a P_{O_2} halfway between two steady-state conditions because, presumably, O_2 flux would be maximum. We estimated D to be 1.3×10^{-6} cm²/s. Our estimated D was smaller than the D calculated from P_{O_2} measurements in 1,000-μm-thick slices of cat cortex equilibrated with a similar initial P_{O_2}, 1.54×10^{-5}cm²/s (21).

Our results suggest that slice $\dot{V}_{O_2}$ was dependent on P_{O_2} of the bathing medium. By assuming that $\dot{V}_{O_2}$ was dependent on P_{O_2}, we approximated $\dot{V}_{O_2}$ from P_{O_2} measurements made at a depth of 150 μm in a brain slice equilibrated with regular aCSF while switching medium P_{O_2} from 708 to 156 or 2,468 Torr. With the same boundary conditions as before, $\dot{V}_{O_2}$ was approximated graphically from the equation (8)

$$\phi(\beta) \approx -P_{O_2} + \left(\frac{2P_1}{\sinh(\beta L)}\right) \sinh\left(\frac{\beta L}{2}\right) + \left[\frac{4P_0}{\pi} - \frac{4\pi P_1}{\pi^2 + (\beta L)^2} \cosh\left(\frac{\beta L}{2}\right)\right] \exp\left[-D\left(\frac{\pi}{L}\right)^2 t\right]$$

where $\phi(\beta) = \beta = \sqrt{\dot{V}/D}$, P_0 is the measured P_{O_2} at a depth of 150 μm into a slice equilibrated with a medium P_{O_2} of 708 Torr, P_1 is the measured P_{O_2} at a depth of 150 μm into a slice equilibrated with either 156 or 2,468 Torr, P_{O_2} is equal to the mean of P_0 and P_1, t is time, in seconds, to reach P_{O_2}, and D is 1.3×10^{-6} cm²/s. To convert $\dot{V}_{O_2}$ to units of milliliters O_2 per cubic centimeters per minute, the approximated $\dot{V}_{O_2}$ was multiplied by the oxygen solubility coefficient of cat brain, 0.0144 ml $O_2 \cdot cm^3$ tissue$^{-1} \cdot$atm^{-1} (21). Switching medium P_{O_2} from 708 to 156 or from 708 to 2,468 Torr resulted in estimated $\dot{V}_{O_2}$ of 7.9×10^{-5} or 7.3×10^{-6} ml $O_2 \cdot cm^3$ tissue$^{-1} \cdot$min^{-1}, respectively.

We acknowledge the assistance of Drs. L. Turyn and T. Svobodny for their help in calculating D and $\dot{V}_{O_2}$, Michael R. Rayle for statistical assistance, Dr. C. Jiang (Georgia State University) for assistance with construction and use of the carbon fiber electrodes, and Phyllis Douglas for technical assistance.

The research was supported, in part, by National Heart, Lung, and Blood Institute Grant R01-HL-56683, Wright State University (WSU) Alpha Grant Program (Kettering Foundation), and the Office of Naval Research Grant N000140110179. D. K. Mulkey was supported by the WSU Biomedical Sciences PhD program.

REFERENCES

1. **Balentine JD.** *Pathology of Oxygen Toxicity*. New York: Academic, 1982.
2. **Bennett P, Papahadjopoulos D, and Bangham A.** The effect of raised pressure of inert gases on phospholipid membranes. *Life Sci* 6: 2527–2533, 1967.
3. **Bingmann D and Kolde G.** Burst activity elicited in hippocampal slices by a rise of P_{O_2}. *Pflügers Arch* 382: R38, 1979.
4. **Bingmann D and Kolde G.** P_{O_2}-profiles in hippocampal slices of the guinea pig. *Exp Brain Res* 48: 89–96, 1982.
5. **Bingmann D, Kolde G, and Speckmann EJ.** Effects of elevated P_{O_2} values in the superfusate on the neural activity in hippocampal slices. In: *Physiology and Pharmacology of Epileptogenic Phenomenon,* edited by Klee MR, Lux HD, and Speckmann EJ. New York: Raven, 1982, p. 97–104.
6. **Brahma B, Forman RE, Stewart EE, Nicholson C, and Rice ME.** Ascorbate inhibits edema in brain slices. *J Neurochem* 74: 1263–1270, 2000.
7. **Brewer GJ and Cotman CW.** Survival and growth of hippocampal neurons in defined medium at low density: advantages of a sandwich culture technique or low oxygen. *Brain Res* 494: 65–74, 1989.
8. **Carslaw HS and Jaeger JC.** *Conduction of Heat in Solids* (2nd ed.). London: Oxford University Press, 1959, p. 99–100.
9. **Cater D, Garattini S, Marina F, and Silver I.** Changes of oxygen tension in brain and somatic tissues induced by vasodilator and vasoconstrictor drugs. *Proc R Soc B* 155: 136–157, 1961.
10. **Cater D, Silver I, and Wilson G.** Apparatus and technique for the quantitative measurement of oxygen tension in living tissues. *Proc R Soc B* 151: 256–276, 1959.
11. **Chance B and Boveris A.** Hyperoxia and hydroperoxide metabolism. In: *Extrapulmonary Manifestations of Respiratory Disease. Lung Biology in Health and Disease,* edited by Robin E. New York: Marcel Dekker, 1978, vol. 8, p. 185–238.
12. **Dean JB and Mulkey DK.** Continuous intracellular recording from mammalian neurons exposed to hyperbaric helium, oxygen, or air. *J Appl Physiol* 89: 807–822, 2000.
13. **Dean JB, Mulkey DK, and Arehart JT.** Details on building a hyperbaric chamber for intracellular recording in brain tissue slices. Supplemental material from *J Appl Physiol*. [online] http://jap.physiology.org/cgi/content/full/89/2/807/DC1.
14. **Dekin MS, Getting PA, and Johnson SMB.** In vitro characterization of neurons in the ventral part of the nucleus tractus solitarius. I. Identification of neuronal types and repetitive firing properties. *J Neurophysiol* 58: 195–214, 1987.
15. **Donnelly D, Jiang C, and Haddad G.** Comparative responses of brain stem and hippocampal neurons to O_2 deprivation: in vitro intracellular studies. *Am J Physiol Lung Cell Mol Physiol* 262: L549–L554, 1992.
16. **Etzion Y and Grossman Y.** Spontaneous Na^+ and Ca^{2+} spike firing of cerebellar Purkinje neurons at high pressure. *Pflügers Arch* 437: 2276–2284, 1999.
17. **Fatt I.** *Polarographic Oxygen Sensors*. Boca Raton, FL: CRC, 1976, p. 63–96, 121–134.
18. **Feldman JL and Ellenberger HH.** Central coordination of respiratory and cardiovascular control in mammals. *Annu Rev Physiol* 50: 593–606, 1988.
19. **Fujii T, Baumgartl H, and Lubbers D.** Limiting section thickness of guinea pig olfactory cortical slices studied from tissue P_{O_2} values and electrical activities. *Pflügers Arch* 393: 83–87, 1982.
20. **Fujii T, Buerk D, and Whalen W.** Activation energy in the mammalian brain slice as determined by oxygen micro-electrode measurements. *Jpn J Physiol* 31: 279–283, 1981.
21. **Ganfield R, Nair P, and Whalen W.** Mass transfer, storage, and utilization of O_2 in cat cerebral cortex. *Am J Physiol* 219: 814–821, 1970.
22. **Gozal D.** Potentiation of hypoxic ventilatory response to hyperoxia in the conscious rat: putative role of nitric oxide. *J Appl Physiol* 85: 129–132, 1998.
23. **Gulati SC, Sood SC, Baili IM, and Kak VK.** Cerebral metabolism following brain injury I Acid-base and P_{O_2} changes. *Acta Neurochir (Wien)* 53: 239–246, 1980.
24. **Hunt R, Blackburn J, Ogilvie R, and Balentine D.** Oxygen tension in the globus pallidus and neostriatum of unanesthetized rats during exposure to hyperbaric oxygen. *Exp Neurol* 62: 698–707, 1978.
25. **Jain KK.** *Textbook of Hyperbaric Medicine*. New York: Kirkland: Hogrefe and Huber, 1996, p. 63–78.
26. **Jamieson D.** Oxygen toxicity and reactive oxygen metabolites in mammals. *Free Radic Biol Med* 7: 87–108, 1989.
27. **Jamieson D and Van den Brenk HAS.** Measurement of oxygen tensions in cerebral tissues of rats exposed to high pressures of oxygen. *J Appl Physiol* 18: 869–876, 1962.

28. **Jiang C, Agulian S, and Haddad G.** O_2 tension in adult and neonatal brain slices under several experimental conditions. *Brain Res* 568: 159–164, 1991.
29. **Kaniuga Z, Bryla J, and Slater E.** Inhibitors around the antimycin-sensitive site in the respiratory chain. In: *Inhibitors, Tools in Cell Research,* edited by Bucher T and Sies H. New York: Springer-Verlag, 1969, p. 282–300.
30. **Kaplan R, Brighton C, Boytim M, Selzer M, Lee V, Spindler K, Silberberg D, and Black J.** Enhanced survival of rat neonatal cerebral cortical neurons at subatmospheric oxygen tensions in vitro. *Brain Res* 384: 199–203, 1986.
31. **Kendig JJ.** Nitrogen narcosis and pressure reversal of anesthetic effects in node of Ranvier. *Am J Physiol Cell Physiol* 246: C91–C95, 1984.
32. **Kohling R, Greiner C, Wolfer J, Wassmann H, and Speckmann E.** Optical monitoring of Po_2 changes and simultaneous recording of bioelectric activity in human and animal brain slices. *J Neurosci Methods* 85: 181–186, 1998.
33. **Kovachich G and Mishra O.** Lipid peroxidation in rat brain cortical slices as measured by the thiobarbituric acid test. *J Neurochem* 35: 1449–1452, 1980.
34. **Kovachich G and Mishra O.** The effect of ascorbic acid on malonaldehyde formation, K^+, Na^+ and water content of brain slices. *Exp Brain Res* 50: 62–68, 1983.
35. **Kramer J, Nolan P, and Waldrop T.** In vitro responses of neurons in the periaqueductal gray to hypoxia and hypercapnia. *Brain Res* 835: 2197–203, 1999.
36. **Krnjevic K.** Early effect of hypoxia on brain cell function. *Croation Med J* 40: 375–380, 1999.
37. **Lehmenkuhler A, Caspers H, and Speckmann EJ.** A method for simultaneous measurements of bioelectric activity and local tissue Po_2 in the CNS. In: *O_2 Transport to Tissue II,* edited by Grote RD, Reneau D, and Theus G. New York: Plenum, 1976, p. 3–7.
38. **Liberzon I, Arieli R, and Kerem D.** Attenuation of hypoxic ventilation by hyperbaric O_2: effects of pressure and exposure time. *J Appl Physiol* 66: 851–856, 1989.
39. **Lipinski H and Bingmann D.** Diffusion in slice preparations bathed in unstirred solutions. *Brain Res* 473: 26–34, 1987.
40. **Lipton P and Whittingham T.** Energy metabolism and brain slice function. In: *Brain Slices,* edited by R. Dingledine. New York: Plenum, 1984, p. 113–153.
41. **Marsden CA, Joseph MH, Kruk ZL, Maidment NT, O'Neill RD, Schenk JO, and Stamford JA.** In vivo voltametry—present electrodes and methods. *Neuroscience* 25: 389–400, 1988.
42. **Mcilwain H.** Introduction: cerebral subsystems as biological entities. In: *Brain Slices,* edited by R. Dingledine. New York: Plenum, 1983, p. 1–5.
43. **Mokashi A and Lahiri S.** Aortic and carotid body chemoreception in prolonged hyperoxia in the cat. *Respir Physiol* 86: 233–243, 1991.
44. **Mulkey DK and Dean JB.** Effects of hyperbaric pressure on membrane potential of solitary complex neurons in rat brainstem slices (Abstract). *FASEB J* 13: A825, 1999.
45. **Mulkey DK and Dean JB.** Hyperbaric pressure and hyperbaric oxygen independently affect membrane potential of solitary complex neurons in rat brainstem slices (Abstract). *FASEB J* 14: A713, 2000.
46. **Mulkey DK, Henderson RA III, and Dean JB.** Hyperbaric oxygen depolarizes solitary complex neurons in tissue slices of rat medulla oblongata. In: *Oxygen Sensing: From Molecule to Man,* edited by Lahiri S, Prabhakar NR, and Forster II RE. New York: Kluwer Academic/Plenum, 2000, chapt. 46, p. 465–476.
47. **Mulkey DK, Henderson RA III, and Dean JB.** Oxygen tension profiles in nucleus tractus solitarius (NTS) in brain slices exposed to normobaric and hyperbaric oxygen (Abstract). *Soc Neurosci Abstr* 26: 425, 2000.
48. **Mulkey DK, Reich JL, and Dean JB.** Comparison of neuronal barosensitivity in the solitary complex to 1 to 8 atmospheres of helium or air (Abstract). *FASEB J* 13: A825, 1999.
49. **Nicoll RA and Madison DV.** General anesthetics hyperpolarize neurons in the vertebrate central nervous system. *Science* 217: 1055–1057, 1982.
50. **Nolan PC and Waldrop TG.** Ventrolateral medullary neurons show age-dependent depolarizations to hypoxia in vitro. *Dev Brain Res* 91: 111–120, 1996.
51. **Oglivie RW and Balentine DJ.** Oxygen tension in spinal cord gray matter during exposure to hyperbaric oxygen. *J Neurosurg* 43: 156–161, 1975.
52. **Okada Y, Mchenhoff K, Holtermann G, Acker H, and Scheid P.** Depth profiles of pH and Po_2 in the isolated brain stem-spinal cord of the neonatal rat. *Respir Physiol* 93: 315–326, 1993.
53. **Parmentier JL, Shrivastav BB, Bennett PB, and Wilson KM.** Effect of interaction of volatile anesthetics and high hydrostatic pressure on central neurons. *Undersea Biomed Res* 6: 75–91, 1979.
54. **Pellmar T.** Electrophysiological correlates of peroxide damage in guinea pig hippocampus in vitro. *Brain Res* 364: 377–381, 1986.
55. **Shibata M and Blatteis CM.** High perfusate Po_2 impairs thermosensitivity of hypothalamic thermosensitive neurons in slice preparations. *Brain Res Bull* 26: 467–471, 1991.
56. **Speckmann EJ, Bingmann D, Lehmenkuhler A, and Lipinski HG.** Changes of the bioelectrical activity and extracellular micromilieu in the central nervous system during variations of local oxygen pressure. In: *Oxygen Sensing in Tissue*, edited by Acker H. New York: Springer-Verlag, 1988, p. 179–191.
57. **Torbati D, Mokashi A, and Lahiri S.** Effects of acute hyperbaric oxygenation on respiratory control in cats. *J Appl Physiol* 67: 2351–2356, 1989.
58. **Van den Brenk HAS and Jamieson D.** Brain damage and paralysis in animals exposed to high pressure oxygen-pharmacological and biochemical observations. *Biochem Pharmacol* 13: 165–182, 1964.
59. **Wann KT and Southan AP.** The action of anesthetics and high pressure on neuronal discharge patterns. *Gen Pharmacol* 23: 993–1004, 1992.
60. **Weast R and Astle MJ** (Eds.). Pressure of aqueous vapor. In*: Handbook of Chemistry and Physics*. Boca Raton, FL: CRC, 1978, vol. 59, p. D232.
61. **Zhang J, Sam A, Klitzman B, and Piantadosi C.** Inhibition of nitric oxide synthase on brain oxygenation in anesthetized rats exposed to hyperbaric oxygen. *Undersea Hyperb Med* 22: 377–382, 1995.